Inorganic Chemistry

Article

pubs.acs.org/IC

Trialkylphosphine-Stabilized Copper(I) Dialkylaluminum(III) Ethanedithiolate Complexes: Single-Source Precursors and a Novel Modification of Copper Aluminum Disulfide

Marcus Kischel, Gregor Dornberg, and Harald Krautscheid*

Institut für Anorganische Chemie, Universität Leipzig, Johannisallee 29, 04103 Leipzig, Germany

Supporting Information

ABSTRACT: Four types of trialkylphosphine-stabilized copper dialkylaluminum ethanedithiolate complexes with the compositions $[{}^{i}Pr_3PCuSC_2H_4SAlR_2]_2$ (R = Me, Et, ${}^{i}Pr$, ${}^{t}Bu$, vinyl), $[({}^{i}Pr_3PCu)_3(SC_2H_4S)_2AlR_2]$ (R = Et), $[(Me_3P)_3CuSC_2H_4SAlR_2]$ (R = Me, Et), and $[(Me_3P)_4Cu][SC_2H_4SAlR_2]$ (R = Me, Et, ${}^{i}Pr$) have been synthesized and structurally characterized by X-ray diffraction. The first series features an eight-membered $(CuSAlS)_2$ ring as the core structure. The trimethylphosphine complexes can be distinguished as nonionic and ionic compounds, depending on the amount of trimethylphosphine. In systematic thermogravimetric studies, the complexes were converted into the ternary semiconductor $CuAlS_2$. In this process, a novel wurtzite-type $CuAlS_2$ phase was identified. Binary copper sulfide is observed as a minor side product in thermolysis reactions when volatile trialkylaluminum is released. The thermolysis reactions are completed at temperatures between 330 and 470 °C, depending on the aluminum alkyls. The Cu/Al ratio and phase purity of the thermolysis products were determined by Rietveld analysis of the powder X-ray diffraction patterns and by inductively coupled plasma optical emission spectroscopy measurements. To our knowledge, this is the first study of molecular single-source precursors for $CuAlS_2$.

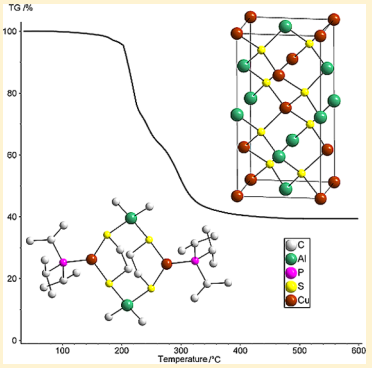

INTRODUCTION

The tetragonal crystal structure of $CuAlS_2$ was first described in a systematic study of $M^{I}M^{III}E_2$ (M^{I} = Cu, Ag; M^{III} = Al, Ga, In, Tl; E = S, Se, Te) compounds by Hahn and co-workers.[1] In the last 2 decades, Harry Hahn phases $CuME_2$ (M = Al, Ga, In; E = S, Se, Te), which crystallize in the tetragonal chalcopyrite structure, have been of great interest because of their potential applications. Such applications include solar cell materials, light-emitting diodes, and nonlinear optical crystals.[2,3] $CuAlS_2$ is a direct semiconductor with a band gap of 3.5 eV, which is the highest value among the chalcopyrite compounds[3] and is known to have promising luminescence properties, making it suitable for light-emitting devices in the blue or ultraviolet range of the spectrum.[4] Furthermore, it features p-type conductivity with potential applications in transparent electronics.[5] Much attention has been given to doping $CuAlS_2$ with various elements of the transition-metal and rare-earth series.[6] Typical synthesis routes include sulfurization of metallic precursors,[7] iodine transport reactions,[8] molecular beam epitaxy,[9] and spray pyrolysis.[10] For other chalocopyrites, e.g., $CuInSe_2$, molecular single-source precursors (SSPs) have been studied intensively, keeping in mind the advantages of deposition under atmospheric pressure, comparably low deposition temperatures, and reliable stoichiometric control.[11] Although SSPs for the generation of $CuAlS_2$ are part of the patent of Hepp et al.,[11] no such complexes have been reported so far. To our knowledge, the first molecular SSPs for $CuAlS_2$ are presented in this paper.

Recently, for several of the $CuME_2$ compounds, a yet-unknown wurtzite-type structure was observed.[12,13] This phase can be regarded as a cation-disordered analogue to the hexagonal zinc sulfide. Both phases, tetragonal and hexagonal, feature tetrahedral coordination of the metal and sulfur atoms. We observed a wurtzite-type modification of $CuAlS_2$ in several samples of $CuAlS_2$ generated by thermolysis.

In this paper, we report the preparation of a series of trialkylphosphine-stabilized copper dialkylaluminum ethanedithiolate complexes and their structural characterization by single-crystal X-ray diffraction. The structural consequences of the different alkyl groups at the aluminum atom and the steric effect of the phosphine ligand are investigated. The nature of the complexes in solution is studied by NMR. In thermogravimetric (TG) experiments, the complexes are converted to the $CuAlS_2$ semiconductor, which is characterized by powder X-ray diffraction and inductively coupled plasma optical emission spectroscopy (ICP-OES), determining the Cu/Al ratio. The TG data and multicore NMR spectra of volatile thermolysis products allow the proposal of a thermolysis reaction mechanism.

RESULTS AND DISCUSSION

1. Synthesis and Product Overview. The herein-reported trialkylphosphine-stabilized copper dialkylaluminum ethanedi-

Received: October 24, 2013
Published: January 22, 2014

   dx.doi.org/10.1021/ic402675w | Inorg. Chem. 2014, 53, 1614−1623

thiolate complexes **3**–**8** and **9a**–**11** can be obtained in good yield by reaction of the trialkylphosphinecopper ethanedithiolate complexes $[^{i}Pr_3PCuSC_2H_4SCuP^{i}Pr_3]_2$[13] (**1**) or $[(Me_3P)_4Cu]_2[Cu_4(SC_2H_4S)_3]$ (**2a**) in toluene with trialkylaluminum and ethanedithiol, followed by crystallization (Scheme 1). A nonpolar, aprotic solvent is necessary for these reactions to prevent the unintended formation of side products. Possible side products include complex **8** with a Cu/Al ratio of 3:1, which was synthesized and characterized in comparison to the other triisopropylphosphine-based complexes. From the molecular structures, the products can be assigned to four structural types, which will be discussed in the following sections.

Scheme 1. Summary of the Reactions

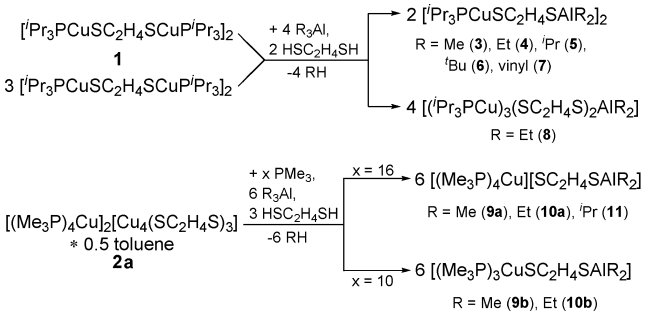

The triisopropylphosphinecopper dialkylaluminum ethanedithiolate complexes **3**–**8** are obtained from toluene. Their solubility in nonpolar solvents decreases with increasing steric demand of the alkyl groups. If the ratio of the starting materials (see Scheme 1) is not balanced, side products like complex **8** will contaminate the product. Under inert conditions, the complexes are stable solids.

The trimethylphosphinecopper ethanedithiolate complex **2a** is prepared by dissolving amorphous copper ethanedithiolate with appropriate amounts of trimethylphosphine in toluene. Copper ethanedithiolate is synthesized by heating copper(I) oxide and ethanedithiol in a mixture of toluene and pyridine. The composition of **2a** is determined by NMR experiments and elemental analysis. Straight from the reaction shown in Scheme 1, complexes **9a**–**11** form oils in toluene and are isolated as microcrystalline powders after crystallization of the oils. Whereas complex **9a** transforms into a microcrystalline powder after several minutes at room temperature, complexes **10a** and **11** are isolated after 24 h at −25 °C as microcrystalline powders. Recrystallization of the isolated complexes **9a** and **10a** from hot toluene leads to single crystals of **9a** and some crystals of **9b** and **10b**, respectively. However, suitable single crystals of complex **10a** could not be obtained. Attempts to synthesize complexes **9b** and **10b** by changing the amount of trimethylphosphine in the reaction were successful, but the isolated products were always mixed with a nonnegligible amount of ionic compounds. Therefore, only ionic complexes were used for thermolysis experiments. The trimethylphosphine complexes are soluble in moderately polar organic solvents, such as tetrahydrofuran (THF) or acetonitrile; in benzene or toluene, they form oils. The complexes are stable solids under inert conditions but decompose within minutes upon contact with air. All complexes presented herein, with copper, aluminum, and sulfur in a molar atomic ratio of 1:1:2, are considered as potential SSPs, which form polycrystalline copper aluminum disulfide upon thermolysis.

2. Molecular Structures. Complexes **3**–**8** share a common structural motif by forming eight-membered rings in their molecular structure with a chairlike conformation. The copper atoms are chelated by ethanedithiolate and coordinatively saturated by one triisopropylphosphine molecule, resulting in a slightly distorted trigonal-planar coordination. The ethanedithiolate ligands are also bridging the dialkylaluminum units in a distorted tetrahedral coordination, which leads to tetranuclear complexes. The aluminum and sulfur atoms are arranged nearly planar, with Al1–S1–S2–Al1′ torsion angles of about 11° or lower. Relevant crystallographic data for complexes **3**–**8** are listed in Table 1; further crystallographic features are described in the Supporting Information (SI; Figures S08–S19 and Table S1).

The molecular structure of complex **3** is shown in Figure 1. In **3**–**8**, the coordination sphere of the copper atom is nearly trigonal-planar, with out-of-plane distances of 3–25 pm. The

Table 1. Crystallographic Data for $[^{i}Pr_3PCuSC_2H_4SAlR_2]_2$ with R = Me (3), Et (4), ^{i}Pr (5), ^{t}Bu (6), and Vinyl (7) and $[(^{i}Pr_3PCu)_3(SC_2H_4S)_2AlEt_2]$ (8)

	3	4	5	6[a]	7	8
chemical formula	$C_{26}H_{62}Al_2Cu_2P_2S_4$	$C_{30}H_{70}Al_2Cu_2P_2S_4$	$C_{34}H_{78}Al_2Cu_2P_2S_4$	$C_{38}H_{86}Al_2Cu_2P_2S_4$	$C_{30}H_{62}Al_2Cu_2P_2S_4$	$C_{35}H_{81}AlCu_3P_3S_4$
fw [g/mol]	745.98	802.08	858.18	914.34	794.02	940.75
space group	$C2/c$ (No. 15)	$P2_1$ (No. 4)	$P\bar{1}$ (No. 2)	$P\bar{1}$ (No. 2)	$P2_1/n$ (No. 14)	$P\bar{1}$ (No. 2)
a [Å]	17.639(2)	11.0435(8)	8.469(2)	8.7529(3)	10.6765(8)	13.549(2)
b [Å]	15.868(2)	15.276(2)	11.733(2)	12.0455(4)	16.498(1)	13.996(2)
c [Å]	15.634(2)	13.215(2)	13.486(2)	13.3844(5)	11.7204(9)	16.075(2)
α [deg]	90	90	65.86(1)	66.073(3)	90	64.164(8)
β [deg]	116.681(5)	107.840(6)	72.63(1)	78.353(3)	95.986(6)	68.421(8)
γ [deg]	90	90	86.59(2)	84.367(3)	90	66.996(8)
V [Å^3]	3910.1(5)	2122.2(3)	1164.1(3)	1263.12(8)	2053.2(3)	2452.6(4)
Z	4	2	1	1	2	2
D_{calc} [g/cm^3]	1.267	1.255	1.224	1.202	1.284	1.274
μ(Mo Kα) [mm^{-1}]	1.443	1.334	1.220	1.144	1.378	1.597
R1 [$I > 2\sigma(I)$]	0.0277	0.0327	0.0236	R_p = 0.0870	0.0312	0.0422
wR2 [all data]	0.0665	0.0689	0.0519	wR_p = 0.1141	0.0803	0.1062
absolute structure parameter		0.46(2)[b]				

[a]Structure solved and refined from powder X-ray diffraction data. [b]Refined as a racemic twin.

dx.doi.org/10.1021/ic402675w | Inorg. Chem. 2014, 53, 1614–1623

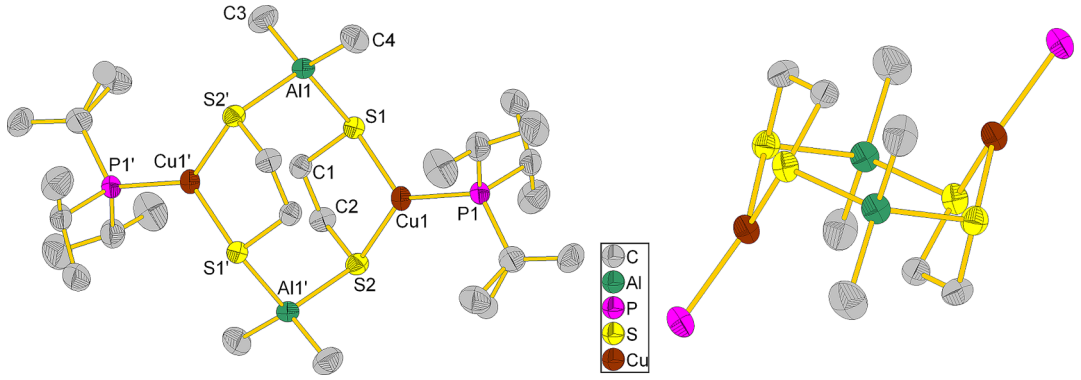

Figure 1. Left: Molecular structure of **3**. Right: Structural motif of the eight-membered ring in chair conformation. Hydrogen atoms are omitted for clarity, and thermal ellipsoids are drawn at the 50% probability level. Symmetry code: ′, 1.5 − *x*, 1.5 − *y*, 1 − *z*.

Cu−S bond lengths vary in the narrow range of 226−233 pm. The aluminum atom is distorted tetrahedrally coordinated, with C−Al−C angles of 116−121° and S−Al−S angles of 110−116°, whereas the Al−S and Al−C distances vary only slightly in the ranges of 230−234 and 196−201 pm, respectively.

The structural motifs of **3**−**7**, as shown in Figure 1, are realized independently of the aluminum dialkyl subunit. Complex **8** with a different ratio of $^{i}Pr_3PCu$ to R_2Al subunits exhibits a closely related motif, with one $^{i}Pr_3PCu$ group replacing an R_2Al unit. Special attention was given to complex **6** because, as a result of the insolubility of the complex in toluene, no single crystals were available. The crystal structure was solved and refined from powder X-ray diffraction data using the method of simulated annealing (see the SI for details). Also, complexes **5** and **6** are isomorphous. Complexes **3** and **5**−**7** feature a center of inversion in the center of the molecule, but in complex **4**, only approximately a center of inversion is present. This is due to a shift of the heavy-atom coordinates and the ethyl groups C5 and C6, which inhibit crystallographic inversion symmetry. Refinement of this structure in a centrosymmetric space group, even considering a disordered ethyl group, was not successful. Structurally similar complexes, containing dialkylgallium and -indium units, have been reported recently, where the Et_2Ga compound shows the same behavior.[14]

The anionic Cu_4S_6 subunit of complex **2a** is already described in the literature with different cations.[15] Because of the bad crystal quality of **2a** grown from toluene, a structure solution only with poor quality was possible. Attempts to recrystallize **2a** from THF yield crystals of $[(Me_3P)_4Cu][Cu_4(SC_2H_4S)_3Cu(PMe)_3]\cdot 1.5THF$ (**2b**), with one trimethylphosphine molecule less than **2a**. Complex **2b** consists of tetrakis(trimethylphosphine)copper cations and tris(ethanedithiolate)tris(trimethylphosphine)pentacuprate anions, as shown in Figure 2. In the tetrahedral Cu_4 subunit of the anion, three copper atoms are chelated by three ethanedithiolate ligands; every sulfur atom is coordinating two copper atoms, resulting in an approximately trigonal-planar CuS_3 coordination sphere with out-of-plane values between 7 and 13 pm. Additionally, one sulfur atom coordinates the tris(trimethylphosphine)copper unit, resulting in a slightly distorted tetrahedral coordination sphere of the copper atom.

The trimethylphosphine-stabilized copper dialkylaluminum ethanedithiolate complexes **9a**−**11** display two distinctive structural motifs, depending on the amount of trimethylphosphine used in the synthesis. Relevant crystallographic data for

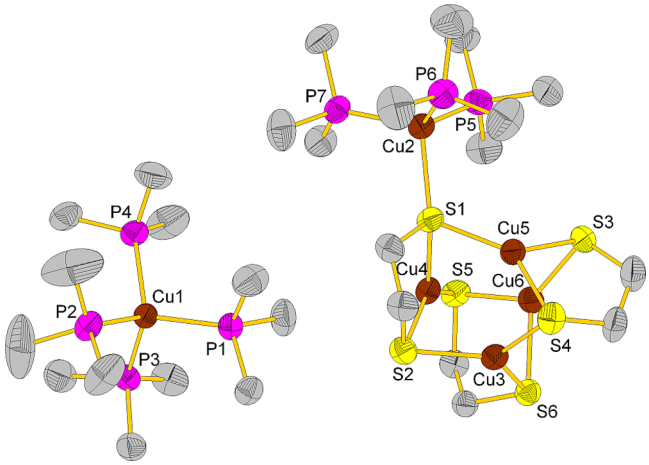

Figure 2. Cation and anion structures of **2b**. Hydrogen atoms and solvent molecules are omitted for clarity, and thermal ellipsoids are drawn at the 50% probability level.

complexes **9a**−**11** are listed in Table 2. Figure 3 shows the molecular structures of complexes **9a** and **9b**. The ionic structural motif, present in the structures of **9a** and **11**, consists of tetrakis(trimethylphosphine)copper cations and ethanedithiolatedialkylaluminate anions. In contrast to **3**−**8**, here the dialkylaluminum unit is chelated by ethanedithiolate, while the copper atom is coordinatively saturated by four trimethylphosphine molecules. Hence, the copper atom features a tetrahedral coordination sphere with P−Cu−P angles between 107° and 111°, whereas the aluminum atom is distorted tetrahedrally coordinated. The C−Al−C angles between 112° and 113° are wider than the S−Al−S angles (97°) and still wider than the ideal tetrahedral angle. This is due to the higher spatial requirements of the covalent Al−C bonds compared to the coordinating Al−S bonds.[16] The tetragonal symmetry of complex **9a** is realized by disorder of the anion, so that the symmetry of a 4-fold inversion axis becomes possible in the center of the anion. Attempts to refine this structure in a lower-symmetry space group did not give any benefits regarding the disorder or the *R* values.

The nonionic structural motif of complexes **9b** and **10b** consists of a chelated dialkylaluminum group of which one sulfur atom is coordinating a tris(trimethylphosphine)copper unit. Again, the copper and aluminum atoms are tetrahedrally coordinated with a certain distortion. While the C−Al−C angles of **9b** and **10b** are in the same range as the angles in the

dx.doi.org/10.1021/ic402675w | *Inorg. Chem.* 2014, 53, 1614−1623

Table 2. Crystallographic Data for 2b, $[(Me_3P)_3CuSC_2H_4SAlR_2]$ with R = Me (9b) and Et (10b), and $[(Me_3P)_4Cu][SC_2H_4SAlR_2]$ with R = Me (9a) and ^{i}Pr (11)

	2b	9a	9b	10b	11
chemical formula	$C_{33}H_{87}Cu_6O_{1.5}P_7S_6$	$C_{16}H_{46}AlCuP_4S_2$	$C_{13}H_{37}AlCuP_3S_2$	$C_{15}H_{41}AlCuP_3S_2$	$C_{20}H_{54}AlCuP_4S_2$
fw [g/mol]	1298.42	517.05	440.98	469.03	573.15
space group	$P\bar{1}$ (No. 2)	$I\bar{4}$ (No. 82)	$Fdd2$ (No. 43)	$P2_1/n$ (No. 14)	$P2_12_12_1$ (No. 19)
a [Å]	12.075(2)	12.943(2)	31.752(3)	10.822(2)	9.3435(9)
b [Å]	14.390(2)	12.943(2)	32.804(3)	16.984(2)	13.917(2)
c [Å]	19.191(2)	8.675(2)	9.3184(9)	14.208(2)	25.887(3)
α [deg]	96.368(8)	90	90	90	90
β [deg]	91.008(8)	90	90	91.901(9)	90
γ [deg]	112.984(7)	90	90	90	90
V [Å^3]	3044.1(5)	1453.3(4)	9706(2)	2610.1(5)	3364.9(6)
Z	2	2	16	4	4
D_{calc} [g/cm^3]	1.416	1.182	1.207	1.194	1.131
μ(Mo Kα) [mm^{-1}]	2.472	1.146	1.298	1.211	0.996
R1 [$I > 2\sigma(I)$]	0.0506	0.0236	0.0421	0.0316	0.0803
wR2 [all data]	0.1364	0.0548	0.0740	0.0705	0.2035
absolute structure parameter		−0.02(2)	0.02(2)		0.01(2)

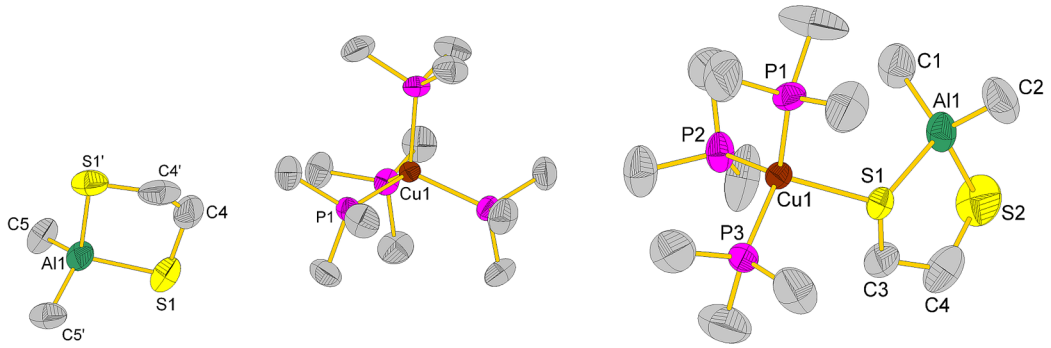

Figure 3. Cation and anion structures of **9a** (left) and structure of **9b** (right). The disorder of **9a** is not displayed. Hydrogen atoms are omitted for clarity, and thermal ellipsoids are drawn at the 50% probability level. Symmetry code: ′, $-x$, $1 - y$, z.

ionic complexes, the S−Al−S angles around 93° are smaller compared to **9a** and **11**. The Al−S bond lengths differ by ca. 4 pm in **9b** and **10b**; the longer bond is due to the bridging sulfur atom.

3. NMR Studies. The triisopropylphosphine-stabilized copper dialkylaluminum ethanedithiolate complexes consist of dimeric units, whereas the trimethylphosphine-stabilized compounds are ionic complexes. To examine the behavior of complexes **3**−**11** in solution, several NMR experiments were conducted. The ^{1}H NMR spectrum of complex **4** in benzene-d_6 shows six signals; the methyl groups of triisopropylphosphine are observed as doublet of doublets, with $^3J_{PH}$ = 14.4 Hz and $^3J_{HH}$ = 7.1 Hz. Also affected by the ^{31}P nucleus, the methine protons appear as a pseudooctet. The signal of the methylene protons of the diethylaluminum unit appears as a multiplet rather than the expected quartet because of the dimeric structure in solution with chemically inequivalent ethyl groups. Furthermore, the ethanedithiolate protons are observed as two multiplet signals with the same intensity but different chemical shifts (2.74 and 3.28 ppm). The coupling constants were determined by simulation on the basis of an AA′BB′ spin system in the five-membered copper ethanedithiolate subunit (Figure 4).

The vicinal coupling constants $^3J_{AA'}$ and $^3J_{BB'}$ were estimated according to the Karplus relationship (Karplus angles 54°/53°) to be 4 Hz, and $^3J_{AB'} = {}^3J_{A'B}$ was 8 Hz (Karplus angle 171°).[17] For the geminal coupling constants $^2J_{AB}$ and $^2J_{A'B'}$, a value of

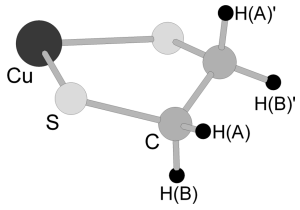

Figure 4. AA′BB′ spin system of the copper ethanedithiolate unit.

−12 Hz was used, in agreement with the literature.[17] Recently reported copper dialkylgallium and -indium ethanedithiolate complexes from our group show the same behavior.[14]

The good agreement between the simulation and the measured spectrum (Figure 5) suggests that the assumption of $^3J_{AB'} = {}^3J_{A'B}$ is correct, consistent with a rapid conformational equilibrium of the dimeric ethanedithiolate chelate unit of complexes **3**−**7** in solution. The ^{31}P{^{1}H} NMR spectrum of complex **4** reveals one signal for triisopropylphosphine, in contrast to complex **1**, which features two broad signals with respect to the two different ^{i}Pr$_3$PCu units. All three signals are observed for complex **8**; from the peak broadening, a fast ligand exchange in solution can be assumed (see the SI, Figure S01).

In the ^{1}H NMR spectrum of complex **8**, all signals assigned to complex **4** can be observed as well, but they appear as broad signals. Figure 6 illustrates the comparison between the ^{1}H NMR spectra of complexes **8**, **1**, and **4** and a stoichiometric

dx.doi.org/10.1021/ic402675w | Inorg. Chem. 2014, 53, 1614−1623

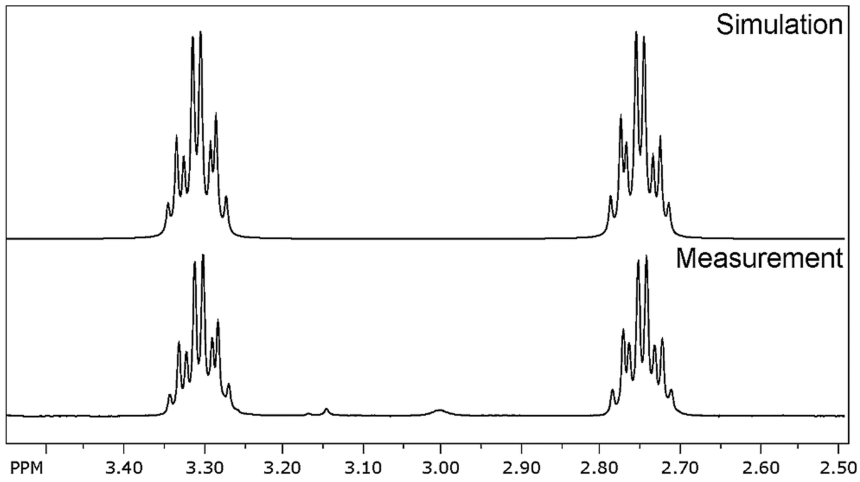

Figure 5. Comparison of the simulated and measured ^{1}H NMR ethanedithiolate signal. Parameters: $^{2}J_{AB} = {}^{2}J_{A'B'} = -12$ Hz, $^{3}J_{AA'} = {}^{3}J_{BB'} = 4$ Hz, $^{3}J_{AB'} = {}^{3}J_{A'B} = 8$ Hz, and line width = 2.0 Hz.

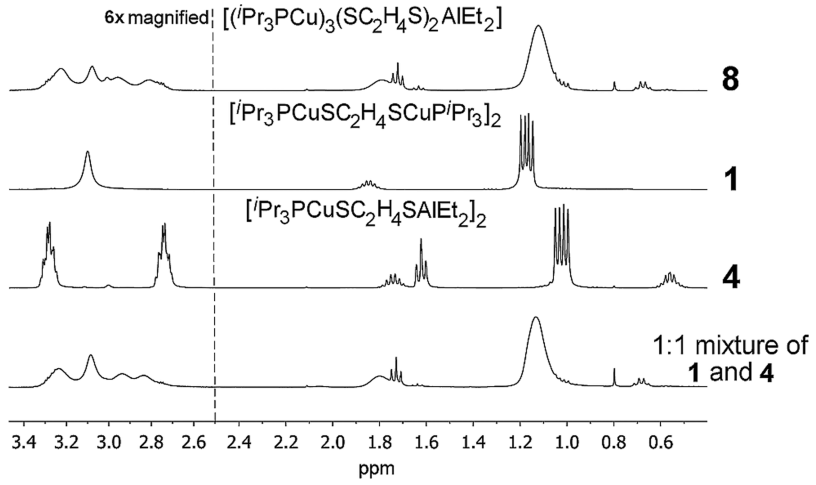

Figure 6. Details of the ^{1}H NMR spectra of complexes **8**, **1**, and **4** and a 1:1 mixture of **1** and **4** in benzene-d_6.

mixture of complex **4** with the starting material **1**. Identification of complex **8** as a side product in the synthesis of **4** is fairly easy, considering the ethanedithiolate signal around 3 ppm and the additional signals in the ^{31}P{^{1}H} NMR spectrum. For **8**, only the signals of the ethyl groups can be observed as multiplets, and the triisopropylphosphine and ethanedithiolate protons appear as broad, partially overlapping singlets, indicating a fast ligand exchange in solution. All signals are shifted downfield in comparison to complex **4**. Additional signals can be observed between the ethanedithiol signals of complex **4**; one matches the signal of complex **1**. Very weak but still visible, a second set of signals from the ethyl groups of the aluminum dialkyl unit is present, matching the original chemical shift of complex **4**.

In summary, complex **8** shows multiple signals assigned to complexes **4** and **1**; the chemical shifts of the triisopropylphosphine signals seem to be averaged between the two compounds. Thus, the equilibrium in Scheme 2 between complex **8** and complexes **4** and **1** is proposed:

The ^{1}H NMR spectra of the ionic complexes **9a**–**11** show sharp singlets for the ethanedithiolate and the methyl groups of trimethylphosphine. A splitting of these signals is not observed at lower temperatures (−20 °C), so conformational exchange in solution is assumed. The ^{31}P{^{1}H} NMR spectra show a quartet signal (1:1:1:1) at −40 ppm with a coupling constant of around 800 Hz. This is an indicator for the presence of the $[(Me_3P)_4Cu]^+$ cation in solution; the quartet originates in a coupling with the ^{63}Cu and ^{65}Cu nuclei ($I = {}^{3}/_{2}$) and a symmetric charge distribution.[18]

Scheme 2. Proposed Equilibrium between Complexes 8, 4, and 1 in Solution

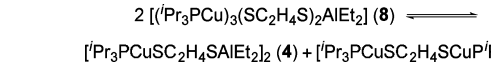

4. Thermolysis Studies. The assumed thermolysis reaction of complexes **3**–**7** is displayed in Scheme 3. Triisopropylphosphine, as a neutral ligand, should leave the complex at temperatures above its boiling point at about 170 °C. The alkyl groups of the aluminum unit are expected to be eliminated as radicals[19] or possibly by β-hydride elimination of the higher

Scheme 3. Proposed Radical Thermolysis Reaction Equation for Complexes 3–7

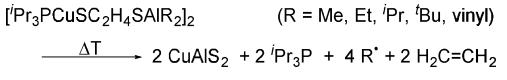

dx.doi.org/10.1021/ic402675w | Inorg. Chem. 2014, 53, 1614–1623

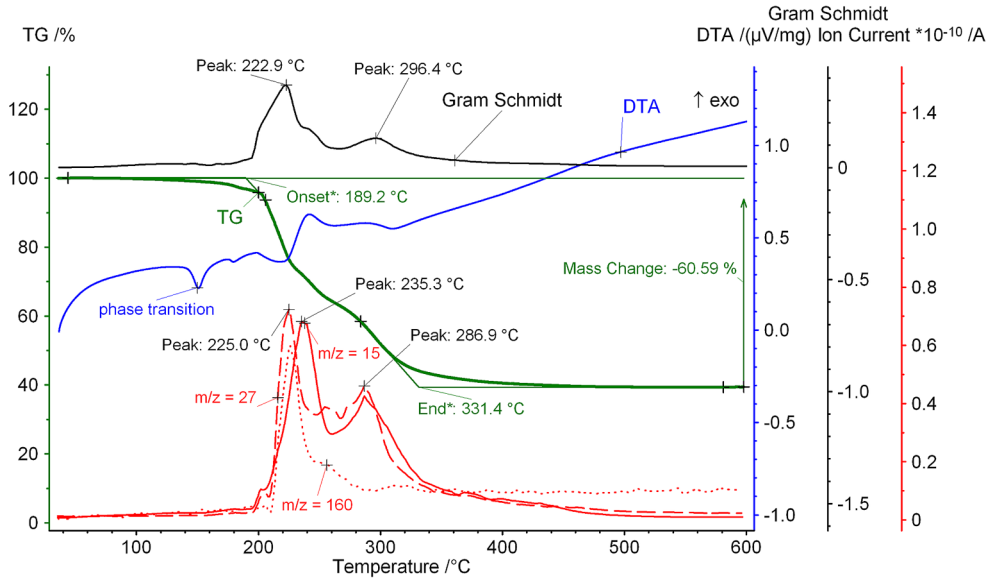

Figure 7. TG, DTA, Gram Schmidt, and ion-current curves of the thermolysis reaction of **3**. Assignment of the *m*/*z* signals: CH_3^+, 15; $C_2H_3^+$, 27, ion current multiplied by a factor of 5; $^iPr_3P^+$, 160, ion current multiplied by a factor of 1000.

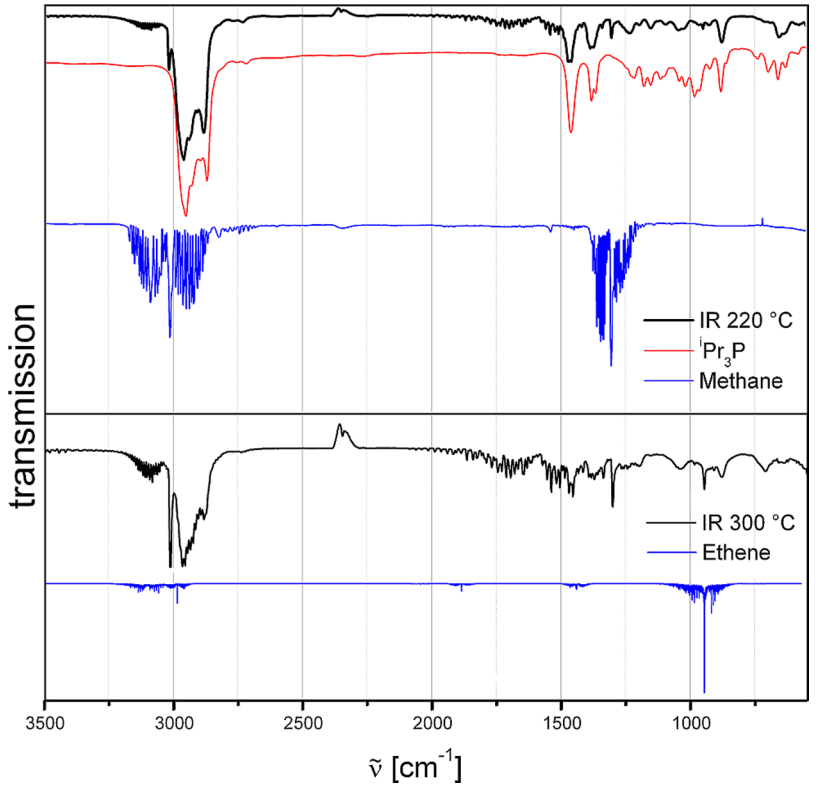

Figure 8. Gas-phase IR spectra of the thermolysis products of **3** at 220 and 300 °C. Database IR spectra of $^iPr_3P$ (Acros Organics), methane (NIST), and ethene (NIST) are shown for comparison.

alkyls.[20] Ethene should be eliminated from the ethanedithiolate unit, allowing the sulfur and metal atoms to form $CuAlS_2$.

In a typical thermolysis experiment, a small amount (25−40 mg) of substance was heated with a heating rate of 10 K/min to 600 °C on a thermobalance coupled to a mass spectrometer and an IR spectrometer. Apart from the TG curve, differential thermal analysis (DTA) curves as well as multiple ion-current curves were detected simultaneously. Exemplary for the triisopropylphosphine precursor system, IR spectra of liberated gaseous compounds were recorded during thermolysis of complex **3**. The onset and end temperatures were determined according to the literature.[21] After thermolysis, powder X-ray diffraction patterns were recorded of the thermolysis residues, and quantitative phase analyses was performed by the Rietveld refinement method. Thermal analysis of complex **3** is reported in Figure 7, and for thermal analysis of complexes **4**−**7** and their Rietveld refinements, see the SI, Figures S23−S26 and S34−S37.

dx.doi.org/10.1021/ic402675w | Inorg. Chem. 2014, 53, 1614−1623

Table 3. Results of the Thermolysis Experiments of Complexes 3−7

	3	4	5	6	7
T_{start} [°C]	189	178	187	192	181
T_{end} [°C]	331	363	385	381	467
mass loss obsd [%]	60.6	62.3	64.2	66.5	59.8
mass loss calcd (Scheme 3) [%]	58.5	61.4	64.0	66.6	61.0
$CuAlS_2$ tetragonal [wt %]	51.0(1)	61.5(2)	67.7(1)	79.6(3)	71.02(8)
$CuAlS_2$ hexagonal [wt %]	43.7(3)	38.5(2)	32.2(3)	17.2(4)	28.9(4)
$Cu_{1.95}S$ [wt %]	5.3(2)				
Cu/Al ratio (Rietveld)	1.11	1	1	1	1
Cu/Al ratio (ICP-OES)	1.20	1.14	1.05	1.06	0.98
residual carbon [%]	1.72	0.75	0.71	0.33	3.15

The TG curve shows a multistep decomposition of **3** between around 180 and 330 °C. The maxima of the ion currents for triisopropylphosphine (m/z 160) and ethene (m/z 27) at 220 °C correlate with the maximum of the Gram Schmidt signal. The maximum ion current for the methane signal (m/z 15) is reached at 240 °C. An IR spectrum of the volatile decomposition products formed at 300 °C (Figure 8) shows signals for methane and ethene, but no more assignable bands for triisopropylphosphine, which is supported by the corresponding ion-current signal. Although cleavage of the methyl groups from the aluminum atom is a radical mechanism, residual moisture leads to the detection of methane in the IR spectra. The overall mass loss of 60.6% is higher than that calculated (58.5%) according to the reaction in Scheme 3, which indicates the loss of a volatile metal species.

According to the Rietveld refinement, the residue consists of 94.7 wt % $CuAlS_2$ and 5.3 wt % $Cu_{1.95}S$ (Digenite), keeping in mind the error of such phase analysis has to be expected in the range of a few percent. To further investigate the thermolysis process, the volatile thermolysis products from an additional experiment with a larger amount of substance were collected in a cold trap cooled with liquid nitrogen. NMR data allow identification of the main compounds (methane, ethene, triisopropylphosphine, and triisopropylphosphine sulfide) and a signal of an unidentified methylaluminum compound in the negative ppm range. Considering the qualitative thermolysis data of **3**, a modified thermolysis reaction taking into account the observed $Cu_{1.95}S$ in the thermolysis residue is proposed, for which the calculated weight loss (60.6%) fits to the experimentally observed value (60.6%). The formation of volatile $AlMe_3$ is responsible for the copper excess in the thermolysis residue, leading to the formation of copper(I) sulfide.

Complexes **4**−**7** show similar thermolysis behavior; the details depend on the alkyl groups R (Table 3). Gaseous products of β-hydride eliminations were not detected; therefore, a radical thermolysis of the R_2Al group is assumed. The binary copper sulfide phase is not present in the diffraction patterns of **4**−**7**, and the experimental mass loss fits to the calculated value quite well. Therefore, the thermolysis reaction should be close to that described by Scheme 3.

Scheme 4. Modified Thermolysis Reaction Equation for Complex 3

$$10\ [{}^{i}Pr_3PCuSC_2H_4SAlMe_2]_2 \xrightarrow[\text{calc. mass loss}\ 60.6\ \%]{\Delta T} 18\ CuAlS_2\ (94.6\ wt\%) + Cu_2S\ (5.4\ wt\%) + 17\ {}^{i}Pr_3P + 3\ {}^{i}Pr_3PS + 2\ AlMe_3 + 34\ CH_3^{\bullet} + 20\ H_2C{=}CH_2$$

According to the Rietveld refinement of the thermolysis residue of **3** (Figure 9), copper aluminum disulfide is present not only as the well-known chalcopyrite type phase but also as the, to our knowledge, not-yet-reported hexagonal wurtzite-type phase. This hexagonal phase of $CuAlS_2$ was refined on the basis of wurtzite-type ZnS, by replacing zinc with equal amounts of copper and aluminum. The lattice constants were refined to a = 373.84(3) pm and c = 617.1(2) pm. The simulated powder X-ray diffractogram of the hexagonal phase in Figure 9 is based on this unit cell.

The occurrence of this hexagonal phase is temperature-dependent. Figure 10 shows temperature-dependent powder X-ray diffraction patterns of thermolysis residues of complex **4** in the range of 50−950 °C. Aside from sharpening of the reflections due to crystallization processes, it is clearly seen that the hexagonal $CuAlS_2$ phase gives way to the tetragonal $CuAlS_2$ phase. This transition occurs fast at temperatures above 600 °C (the time for one temperature step including measuring time is 15 min). No distinct reflections of the hexagonal phase are visible above 750 °C.

A comparison of the thermolysis data (Table 3) shows that, with increasing size of the alkyl group, the end temperature of thermolysis also increases, by the amount of hexagonal $CuAlS_2$ decreases in the series of complexes. The copper(I) sulfide phase can only be observed in significant amounts by Rietveld refinement of the residue of complex **3**.

ICP-OES measurements of the residues (see the SI, Table S2) are in reasonable agreement with the Rietveld data, considering the uncertainty of phase fraction determination by powder diffraction. Especially, the residues of **5**−**7** show nearly equal molar amounts of copper and aluminum. The vinyl-aluminum derivative **7** seems to behave differently from the series of saturated alkyls; it is the only one with a mass loss lower than that calculated and a higher end temperature of thermolysis, indicating the formation of elemental carbon from the unsaturated alkyl groups. This is confirmed by elemental analysis of the residues. The carbon content of the other residues is less than 1% (except **3**) and decreases with increasing size of the aluminum alkyl unit.

In general, the size of the alkyl groups correlates with the thermolysis end temperature and formation of the hexagonal $CuAlS_2$ phase. The formation of $Cu_{1.95}S$ seems to be dependent on the boiling point of the trialkylaluminum compound. Trimethylaluminum with a boiling point of 125 °C can easily be evaporated during thermolysis immediately after its formation. Triethylaluminum, in contrast, has a boiling point of 197 °C (1 atm), which is in the range of the decomposition temperature. The higher trialkylaluminum compounds have even higher boiling points, or experience decomposition before

dx.doi.org/10.1021/ic402675w | Inorg. Chem. 2014, 53, 1614−1623

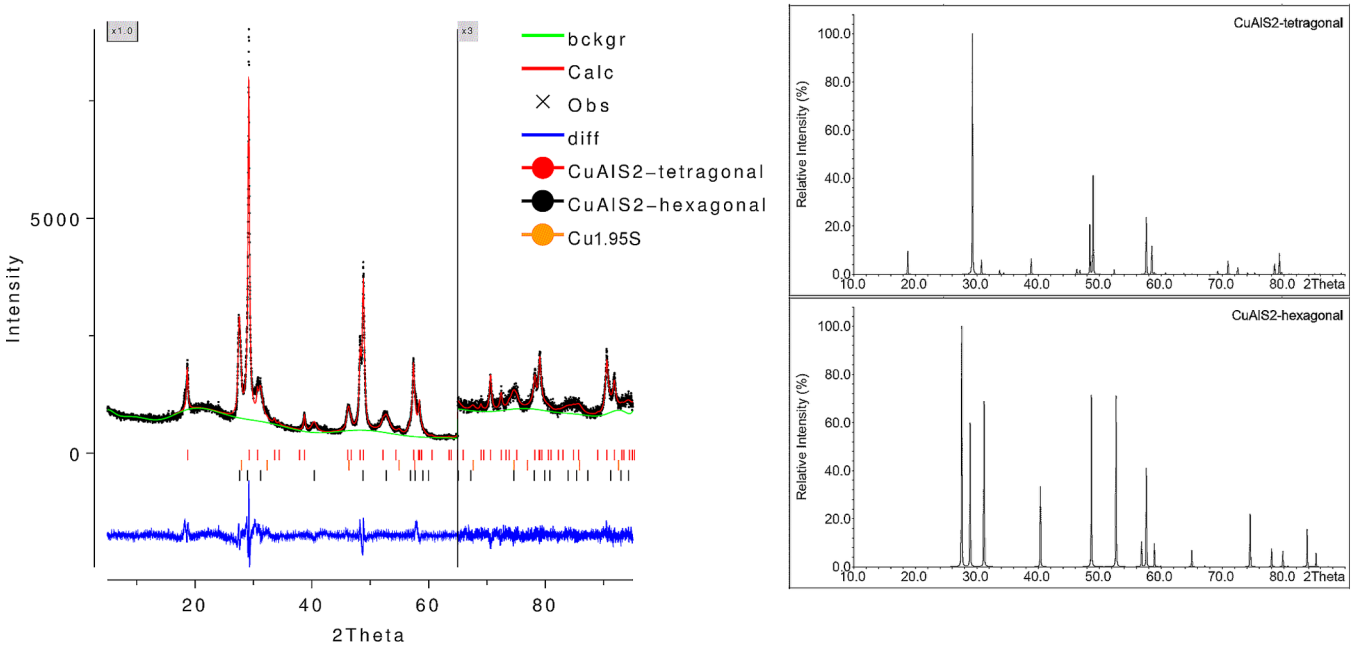

Figure 9. Rietveld refinement plot of the thermolysis residue of **3**. R_p = 0.0527, wR_p = 0.0677, and $R(F^2)$ = 0.0395 (left). Simulated powder X-ray diffractograms of tetragonal and hexagonal $CuAlS_2$ (left).

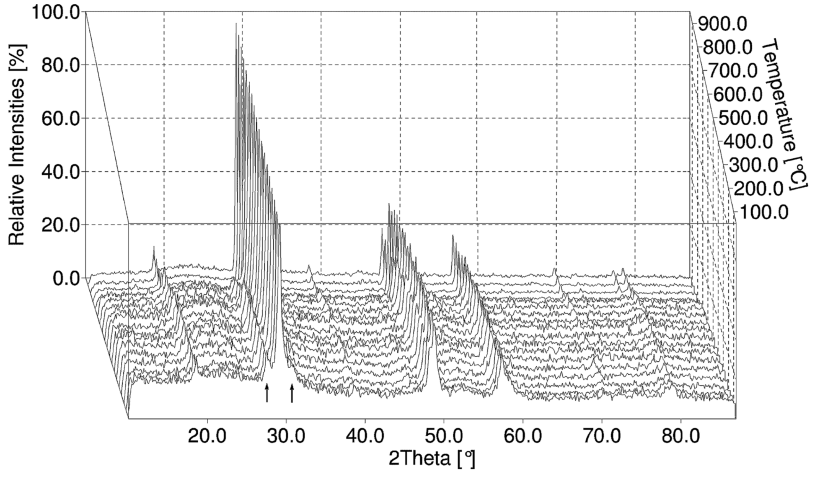

Figure 10. Temperature-dependent powder X-ray diffraction patterns of the thermolysis residue of **4** in the range of 50–950 °C. The intensities are normalized, and the strongest reflections of hexagonal $CuAlS_2$ are marked.

boiling under normal pressure. This is the reason why copper(I) sulfide is not observed in the powder diffraction patterns of the thermolysis residues of complexes **4**–**7**.

The thermolysis reactions of the ionic complexes **9a**–**11** are expected to be similar to those of the triisopropylphosphine-based complexes **3**–**8** and are shown in Scheme 5.

The results of thermal analysis of the ionic complex **9a** are shown in Figure 11. For thermal analysis of complexes **10a** and **11** and the Rietveld refinements of the thermolysis residues, see the SI, Figures S31–S32 and S38–S40. Thermolysis takes place between 80 and 360 °C and starts with the loss of PMe_3. The corresponding ion-current and Gram Schmidt graphs (see the SI, Figure S28–S30) suggest a release of PMe_3 at 80–140 and 160–230 °C. Above 230 °C, no more PMe_3 is detected; however, methane besides a small signal of ethene is prominent in the IR spectrum and the ion-current graph around 250 °C. At about 380 °C, no more significant signals of methane are detected in the IR spectra. Ethene, besides methane, becomes clearly visible in the IR spectrum at 280 °C and is also detected by the ion-current maxima at 290 °C, fading at 350 °C.

A cold-trap thermolysis experiment with **9a** leads to identification of methane, ethene, trimethylphosphine, trimethylphosphine sulfide, and ethylene sulfide and an unidentified methylaluminum species with an ^1H NMR signal at −1 ppm. The mass loss of complex **9a** is in good agreement with the calculated value according to Scheme 5, yet the Rietveld refinement of the thermolysis residue reveals 14 wt % $Cu_{1.95}S$ (Digenite) as the side product. With respect to $CuAlS_2$, ICP-OES data also show a clear excess of copper in this thermolysis

Scheme 5. Proposed Radical Thermolysis Reaction Equation for Complexes 9a–11

$$[(Me_3P)_4Cu][SC_2H_4SAlR_2] \quad (R = Me, Et, {}^iPr)$$
$$\xrightarrow{\Delta T} CuAlS_2 + 4\,PMe_3 + 2\,R^{\bullet} + H_2C{=}CH_2$$

dx.doi.org/10.1021/ic402675w | Inorg. Chem. 2014, 53, 1614–1623

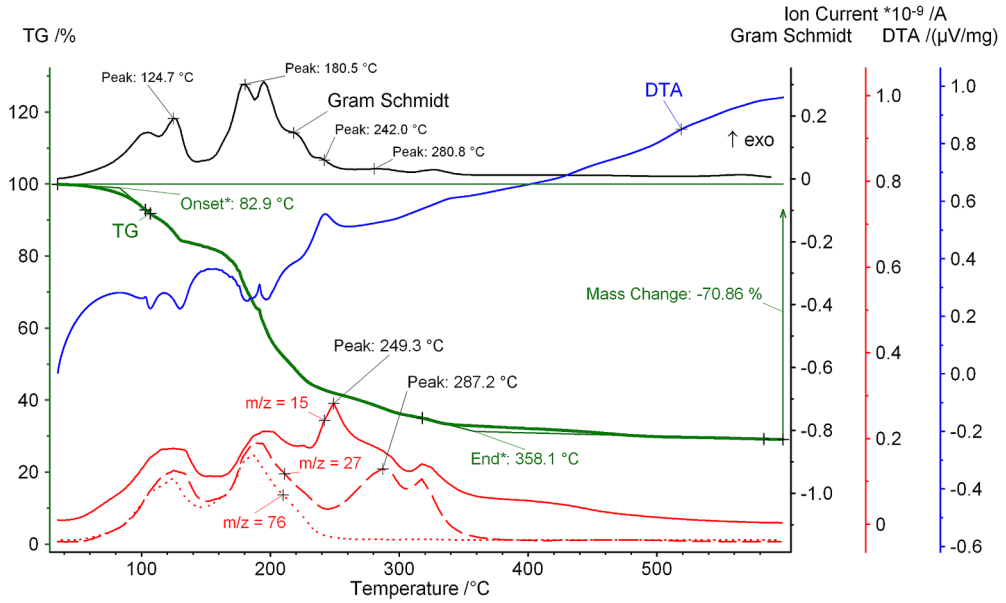

Figure 11. TG, DTA, Gram Schmidt, and ion-current curves of the thermolysis reaction of **9a**. Assignment of the *m*/*z* signals: CH_3^+, 15; $C_2H_3^+$, 27; Me_3P^+, 76, ion current multiplied by a factor of 10.

residue (Table 4). On the basis of the collected data, the thermolysis reaction is modified in Scheme 6 for complex **9a**:

Scheme 6. Modified Thermolysis Reaction Equation for Complex 9a

$$7\ [(Me_3P)_4Cu][SC_2H_4SAlMe_2]\ (\mathbf{9a}) \xrightarrow[\text{calc. mass loss 74.2 \%}]{\Delta T} 5\ CuAlS_2 + Cu_2S + 26\ PMe_3 + 2\ SPMe_3 + H_4C_2S + 2\ AlMe_3 + 8\ CH_3^{\bullet} + 6\ H_2C{=}CH_2$$

(82.9 wt% 17.1 wt%)

In contrast to the thermolysis of complex **3**, the excess sulfur is released as trimethylphosphine sulfide and also as ethylene sulfide. Thermal analyses of **10a** and **11** show the same characteristics, except for the amount of the copper sulfide phase. Table 4 presents the results of the thermolysis experiments of complexes **9a**–**11**.

Table 4. Results of the Thermolysis Experiments of Complexes 9a–11

	9a	10a	11
T_{start} [°C]	83	78	96
T_{end} [°C]	358	340	332
mass loss obsd [%]	70.9	70.5	71.1
mass loss (Scheme 5) [%]	70.1	71.6	73.0
$CuAlS_2$ tetragonal [wt %]	86.0(4)	(100)[a]	100
$Cu_{1.95}S$ [wt %]	14.0(3)		
Cu/Al ratio (Rietveld)	1.32	(1)	1
Cu/Al ratio (ICP-OES)	1.33	1.23	1.10
residual carbon [%]	2.18	1.95	1.80

[a]Small amounts of $Cu_{1.95}S$ identified.

The onset temperatures for complexes **9a**–**11** are in the same range, while the end point slightly decreases with increasing size of the alkyl groups. Again cleavage of the alkyl groups from the aluminum atom is the limiting step for the end point of thermolysis. The amount of residual carbon (ca. 2%) is higher compared to the triisopropylphosphine complexes. The residue of complex **10a** shows the reflections of the $Cu_{1.95}S$ phase, but because of the low intensity, it cannot be quantified by Rietveld refinement. Cu/Al ratios determined by ICP-OES suggest an amount comparable to that in the residue of complex **3** (approximately 5% $Cu_{1.95}S$). Complex **11** yields $CuAlS_2$ without additional crystalline phases; the Cu/Al ratio shows just a slight excess of copper. Therefore, the thermolysis behavior of complex **11** is in good agreement with the reaction equation displayed in Scheme 5. The novel hexagonal wurtzite-like $CuAlS_2$ phase is not present in the thermolysis residues of the ionic complexes.

SUMMARY AND CONCLUSIONS

A total of nine trialkylphosphine-stabilized copper dialkylaluminum ethanedithiolate complexes were isolated and characterized by X-ray diffraction. The triisopropylphosphine complexes $[^iPr_3PCuSC_2H_4SAlR_2]_2$ (**3**–**7**; R = Me, Et, ^{i}Pr, ^{t}Bu, vinyl) and $[(^iPr_3PCu)_3(SC_2H_4S)_2AlR_2]$ (**8**; R = Et) feature an eight-membered ring of the heavy atoms as the core structure. The trimethylphosphine complexes $[(Me_3P)_4Cu][SC_2H_4SAlR_2]$ (**9a** and **11**; R = Me, ^{i}Pr) and $[(Me_3P)_3CuSC_2H_4SAlR_2]$ (**9b** and **10b**; R = Me, Et) form ionic or nonionic compounds, depending on the amount of trimethylphosphine used in the synthesis. In total, four different structural motifs can be distinguished from the molecular structures of these complexes. The different structural motifs originate from the different steric demands of the trialkylphosphines expressed in the Tolman cone angle. The behavior of all complex types in solution was studied by NMR experiments. These experiments lead to the conclusion that complexes **3**–**7** are dimeric in solution as well as in their solid-state structure. A series of simultaneous TG experiments with mass spectrometry and IR coupling are presented and combined with identification of the volatile thermolysis products by NMR spectroscopic data. This allows a proposal of thermolysis reactions for both triisopropyl- and trimethylphosphine complexes. In general, the thermolysis process starts with the release of the phosphine ligand, overlapping followed by elimination of ethene from ethanedithiolate and elimination of the aluminum alkyl groups, which is the final step determining the thermolysis end

dx.doi.org/10.1021/ic402675w | Inorg. Chem. 2014, 53, 1614–1623

temperature. Thermolysis leads to the semiconductor $CuAlS_2$ in all cases. The release of volatile trialkylaluminum is responsible for the occurrence of binary copper sulfide impurities in the thermolysis residues of complexes **3**, **9a**, and **10a**. The Cu/Al ratio in the residues determined by ICP-OES measurements are in reasonable agreement with the calculated ratios based on the Rietveld refinements. It was found that bulkier aluminum alkyls improve the purity of the obtained $CuAlS_2$ but also raise the end temperature of the thermolysis reaction in the case of triisopropylphosphine complexes. In the thermolysis residues of complexes **3**–**7**, a novel phase of $CuAlS_2$ is present after thermolysis, which was identified and refined as hexagonal copper aluminum disulfide. This phase is related to the wurtzite structure, with Cu^+ and Al^{3+} sharing the cation positions. Investigations of chalcopyrite and wurtzite type $CuAlS_2$ particles are in progress.

■ ASSOCIATED CONTENT

Supporting Information

Synthesis and crystallographic information of **1**–**11**, NMR spectra of complexes **8**, **1**, and **4**, a 1:1 mixture of **1** and **4**, and the cold trap experiments of **3** and **9a**, thermal analysis of **3**–**7** and **9a**–**11**, Rietveld refinements of the residues, and ICP-OES data. This material is available free of charge via the Internet at http://pubs.acs.org. CCDC 967917–967926 contain the supplementary crystallographic data for this paper. These data can be obtained free of charge from The Cambridge Crystallographic Data Centre via www.ccdc.cam.ac.uk/data_request/cif.

■ AUTHOR INFORMATION

Corresponding Author

*E-mail: krautscheid@rz.uni-leipzig.de.

Notes

The authors declare no competing financial interest.

■ ACKNOWLEDGMENTS

We thank Dr. H.-J. Stärk and co-workers from the Helmholtz Center for Environmental Research (UFZ Leipzig, Germany) for ICP-OES measurements. Financial support by the University of Leipzig (PbF1) is gratefully acknowledged.

■ REFERENCES

(1) Hahn, H.; Frank, G.; Klingler, W. *Z. Anorg. Allg. Chem.* **1953**, *271*, 153–170.

(2) (a) Paorici, C.; Zanotti, L. *Mater. Chem.* **1980**, *5*, 337–352. (b) Kuroki, Y.; Kato, A.; Okamoto, T.; Takata, M. *J. Electroceram.* **2008**, *21*, 378–380. (c) Shay, J. L.; Tell, B.; Kasper, H. M. *Appl. Phys. Lett.* **1971**, *19*, 366. (d) Bairamov, B. H.; Aydinli, A.; Bodnar, I. V.; Rud, Y. V.; Nogoduyko, V. K.; Toporov, V. V. *J. Appl. Phys.* **1996**, *80*, 5564–5569.

(3) Bhar, G. C.; Smith, R. C. *Phys. Status Soilidi A* **1972**, *13*, 157–168.

(4) Aksenov, I.; Sato, K. *Appl. Phys. Lett.* **1992**, *61*, 1063–1065.

(5) Huang, F.-Q.; Liu, M.-L.; Yang, C. *Sol. Energy Mater. Sol. Cells* **2011**, *95*, 2924–2927.

(6) (a) Aksenov, I.; Kai, T.; Nishikawa, N.; Sato, K. *Jpn. J. Appl. Phys.* **1993**, *32*, 516–519. (b) Huang, D.; Zhao, Y.-J.; Tian, R.-Y.; Chen, D.-H.; Nie, J.-J.; Cai, X.-H.; Yao, C.-M. *J. Appl. Phys.* **2011**, *109*, 113714. (c) Liu, M.-L.; Huang, F.-Q.; Chen, L.-D.; Wang, Y.-M. *Appl. Phys. Lett.* **2007**, *90*, 072109–1–072109–4. (d) Nishi, T.; Kimura, Y.; Sato, K. *J. Lumin.* **2000**, *87–89*, 1105–1107. (e) Sarkisov, S. Y.; Picozzi, S. *J. Phys.: Condens. Matter* **2007**, *19*, 16210. (f) Shim, Y.; Hasegawa, K.; Wakita, K.; Mamedov, N.; Yamamoto, N. *Phys. Status Solidi C* **2009**, *6*, 1089–1092. (g) Zhao, Y.-J.; Zunger, A. *Phys. Rev. B* **2004**, *69*, 1–7.

(7) Bhandari, R. K.; Hashimoto, Y.; Ito, K. *Jpn. J. Appl. Phys.* **2004**, *43*, 6890–6893.

(8) Kuroki, Y.; Okamoto, T.; Ohara, S.; Takata, M. *Key Eng. Mater.* **2004**, *269*, 95–98.

(9) Morita, Y.; Narusawa, T. *Jpn. J. Appl. Phys.* **1992**, *31*, 1396–1398.

(10) Caglar, M.; Ilican, S.; Caglar, Y. *Opt. Commun.* **2008**, *281*, 1615–1624.

(11) (a) Banger, K. K.; Hepp, A. F.; Harris, J. D.; Jin, M. H.; Castro, S. L. U.S. Patent 6,992,202 B1, Jan 31, 2006. (b) Hirpo, W.; Dhingra, S.; Sutorik, A. C.; Kanatzidis, M.-G. *J. Am. Chem. Soc.* **1993**, *115*, 1597–1599.

(12) (a) Huang, W.-C.; Tseng, C.-H.; Chang, S.-H.; Tuan, H.-Y.; Chiang, C.-C.; Lyu, L.-M.; Huang, M. H. *Langmuir* **2012**, *28*, 8496–8501. (b) Wang, Y.-H. A.; Zhang, X.; Bao, N.; Lin, B.; Gupta, A. *J. Am. Chem. Soc.* **2011**, *133*, 11072–11075.

(13) Kluge, O.; Friedrich, D.; Wagner, G.; Krautscheid, H. *Dalton Trans.* **2012**, *41*, 8635–8642.

(14) Friedrich, D.; Kluge, O.; Kischel, M.; Krautscheid, H. *Dalton Trans.* **2013**, *42*, 9613–9620.

(15) (a) Baumgartner, M.; Schmalle, H.; Dubler, E. *Inorg. Chim. Acta* **1993**, *208*, 135–143. (b) Henkel, G.; Krebs, B.; Betz, P.; Fietz, H.; Saatkamp, K. *Angew. Chem., Int. Ed. Engl.* **1988**, *27*, 1326–1329.

(16) Haaland, A. *Angew. Chem., Int. Ed. Engl.* **1989**, *28*, 992–1007.

(17) Hesse, M.; Meier, H.; Zeeh, B. *Spektroskopische Methoden in der organischen Chemie*; Thieme: Stuttgart, Germany, 2002.

(18) (a) Asaro, F.; Camus, A.; Gobetto, R.; Olivieri, A. C.; Pellizer, G. *Solid State Nucl. Magn. Reson.* **1997**, *8*, 81–88. (b) Berger, S.; Braun, S.; Kalinowski, H.-O. *NMR-Spektroskopie von Nichtmetallen. Band 3: ^{31}P-NMR-Spektroskopie*; Georg Thieme Verlag: Stuttgart, Germany, 1993.

(19) Yeddanapalli, L. M.; Schubert, C. C. *J. Chem. Phys.* **1946**, *1*, 1–7.

(20) Smith, W. L.; Wartik, T. *J. Inorg. Nucl. Chem.* **1967**, *29*, 629–645.

(21) Cammenga, H. K.; Epple, M. *Angew. Chem., Int. Ed. Engl.* **1995**, *34*, 1171–1187.